Extreme UV Radiation Grafting of Glycidyl Methacrylate Nanostructures onto Fluoropolymer Foils by RAFT-Mediated Polymerization

Patrick Farquet,[†] Celestino Padeste,*[,†] Harun H. Solak,[†] Selmiye Alkan Gürsel,[‡] Günther G. Scherer,[‡] and Alexander Wokaun[‡]

Laboratory of Micro- and Nanotechnology and Laboratory of Electrochemistry, Paul Scherrer Institut, 5232 Villigen PSI, Switzerland

Received January 28, 2008; Revised Manuscript Received June 24, 2008

ABSTRACT: Periodic nanostructures of poly(glycidyl methacrylate) (pGMA) were grafted onto poly(ethylene-*alt*-tetrafluorethylene) (ETFE) films by reversible addition−fragmentation chain transfer (RAFT) polymerization. ETFE samples were first irradiated in an interference lithographic setup using EUV (extreme ultraviolet) light followed by exposure to air to introduce surface peroxide groups serving as thermal initiators for the graft polymerization. The dependence of height and morphology of the grafted pGMA structures on the exposure dose and on the grafting parameters such as time and concentration of RAFT chain transfer agent was studied with atomic force microscopy (AFM) and scanning electron microscopy (SEM). RAFT mediation reduces the grafted layer thickness by a factor of 5−10 compared to uncontrolled free radical polymerization and significantly improves the spatial resolution into the 50 nm range. A mushroom to brush transition was observed for low absorbed doses. This transition was found to occur at $\sim(1.5 \pm 0.7) \times 10^{-3}$ and $\sim(3 \pm 1.3) \times 10^{-3}$ chains/nm^2 for the free radical and RAFT-mediated polymerization, respectively. The grafting density increased with increasing absorbed dose up to a maximum of 0.1−0.2 chains/nm^2. The data interpretation is supported by simulations based on photon statistics.

Introduction

Polymer brushes are dense arrays of end-tethered polymer chains attached to a surface, which are forced to stretch away from the surface due to dense packing.[1] During the past several decades the interest in theoretical understanding[2−8] as well as practical applications of such systems has grown steadily. Polymer brushes enable the tuning of the surface properties, by physical and/or chemical modification in order to get specific surface characteristics[9−12] or by controlled morphological changes induced by external stimuli such as changes in solvents, pH, or temperature.[13,14] The usual ways to create polymer brushes include polymerization from an initiator bound to oxide surfaces[15−17] or from initiating sites created by radiation on polymer surfaces.[18−20] Radiation grafting with X-rays, UV, e-beam, or plasma particles to create initiating sites in defined area has been performed on many different types of polymers, but only in recent years the attention was focused on fluoropolymers.[18] This polymer family is of interest because of its low surface energy, its bioinactivity, and its high chemical and mechanical stability.

Controlled living radical polymerization (LRP) based on the equilibrium between dormant species and growing ends, such as nitroxide-mediated polymerization,[21−24] atom transfer radical polymerization (ATRP or reverse ATRP),[17,25−27] and reversible addition−fragmentation chain transfer polymerization (RAFT),[28−30] enables better control on the absolute length and length distribution of polymer chains compared to free radical polymerization. Among these LRP, one of the most versatile is RAFT polymerization because of its ability to polymerize a large range of monomers and to reach a controlled molecular weight and architecture. Addition of defined quantities of a chain transfer agent (CTA) into the polymerization solution allows controlling the length of the grafted chain due to the high frequency of CTA transfers between growing ends and dormant polymer chains. Furthermore, polymer chains end-capped with CTA can be isolated from the solution and used to start the grafting of another polymer, eventually resulting in block copolymers. Combining the recent advances in LRP methods and in patterning technology is a promising way to obtain well-defined micro- and nanostructured polymer brushes for future applications in optics, (bio)sensorics, fluidics, and organic electronics.[31−37]

Radiation grafting based on extreme ultraviolet (EUV) interference lithographic exposures is a novel technique to create micro- or nanopatterns of polymer brushes on fluoropolymers. This lithographic grafting process can be applied to many combinations of polymer supports and grafted monomers enabling the preparation of a great variety of functional polymer structures with selected properties.[38] EUV light with an ionizing photon energy in the range of 100 eV has a low penetration (attenuation length <100 nm) in polymeric materials and is utilized to create high-resolution patterns.[39] In this work, this ionizing radiation is used to perform lithographic exposures of polymer samples in order to create radical patterns near the polymer surface. Radicals are then transformed into peroxides and hydroperoxides when they are brought into contact with air and used as thermal initiators for the subsequent graft polymerization. Here we report on grafting nanostructures of poly(glycidyl methacrylate) (pGMA) by RAFT-mediated polymerization onto flexible films of poly(ethylene-*alt*-tetrafluorethylene) (ETFE) using the preformed peroxides as thermal initiating sites (Figure 1). The reactions of pGMA epoxy moieties enable the synthesis of nanostructures with desired functionalities.[40] The aim of this work is to show the effect of RAFT-mediated polymerization and the effect of the exposure dose on resolution of grafted nanostructure patterns. The experimental data are supported by simulated EUV intensity profiles to explain the main processes involved, such as grafting density and critical mushroom to brush transition.

* Corresponding author: e-mail celestino.padeste@psi.ch; Ph +41563102141; Fax +41563102646.
[†] Laboratory of Micro- and Nanotechnology.
[‡] Laboratory of Electrochemistry.

10.1021/ma800202b CCC: $40.75
Published on Web 08/15/2008

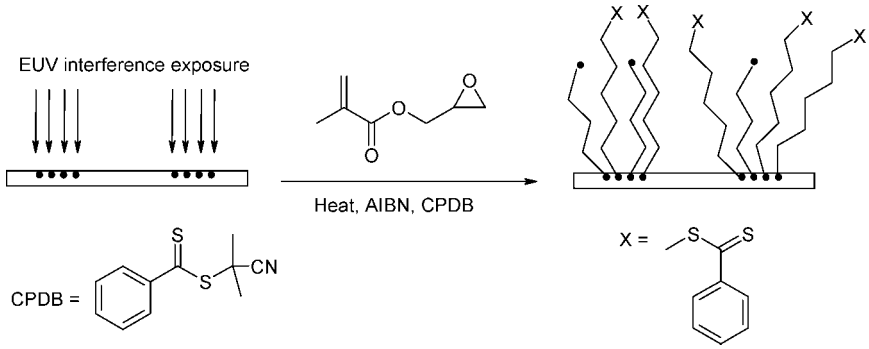

Figure 1. Diagram showing the structure formation: fluoropolymer substrates are exposed to extreme ultraviolet (EUV) radiation. The subsequent RAFT-mediated graft polymerization of glycidyl methacrylate is performed with α,α′-azoisobutyronitrile (AIBN) as the initiator and cyanoisopropyl dithiobenzoate (CPDB) as the chain transfer agent.

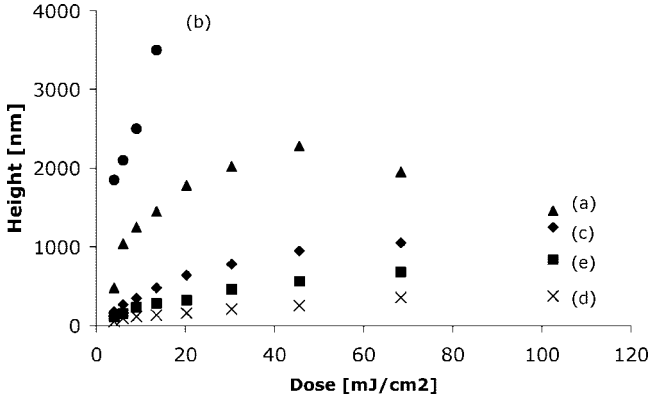

Figure 2. Dose height chart for graft polymerization of glycidyl methacrylate (30 vol %) in methyl ethyl ketone onto poly(ethylene-*co*-tetrafluoroethylene) foils exposed with extreme ultraviolet light: ▲ (a): free radical polymerization for 0.5 h; ● (b): free radical polymerization for 1 h with 1 mM α,α′-azo-isobutyronitrile (AIBN); ◆ (c): RAFT-mediated polymerization in 1 mM of AIBN and 7.5 mM of cyanoisopropyl dithiobenzoate (CPDB) for 1 h; × (d): with 15 mM of CPDB for 1 h and ■ (e) for 2 h.

Experimental Section

Materials. Extruded 100 μm thick films of ETFE (Nowoflon ET-6235 Nowofol GmbH, Siegsdorf, Germany) were placed between two polished 4 in. silicon wafers and hot pressed for 5 min at 230 °C with a pressure of 200 N/cm^2 in order to obtain flat surfaces.

Glycidyl methacrylate (GMA, Fluka, p.a) was vacuum-distilled before the grafting reactions. α,α′-Azo-isobutyronitrile (AIBN, Fluka, purum), methyl ethyl ketone (MEK, Merck), isopropanol (Fischer), and acetone (Fischer) were used as received.

The RAFT agent, cyanoisopropyl dithiobenzoate (CPDB), was synthesized according to the method described by Duréault et al.,[41] by reacting phosphorus pentasulfide (Aldrich), AIBN, and benzoic acid (Fluka) in toluene (Merck). The product was purified by chromatography. All the reactants for the synthesis of CPDB were used without any prior treatments.

Exposure. EUV exposures were performed in vacuum ($<10^{-5}$ mbar) at the XIL beamline of the Swiss Light Source. The beamline uses undulator light with a central wavelength of 13.4 nm (92.5 eV) and ∼3% spectral bandwidth. The samples were irradiated using diffraction grating masks according to methods described earlier.[42] The gratings on the mask diffract EUV light into various orders. Zeroth-order diffraction (directly transmitted beam) is used to expose areas of the sample with uniform intensity whereas interference fringes formed by first-order diffracted beams are used to expose areas of the samples with a sinusoidally varying intensity distribution. The beam intensity is measured by a photodiode placed before the mask. Exposure dose is controlled by a fast beam shutter. The dose delivered to the sample (polymer foil) is calculated using data obtained from diffraction efficiency measurements and the dose delivered to the mask. Irradiated samples were exposed to air and stored in a deep freezer (−80 °C) until further processing.

Table 1. Size Exclusion Chromatographic Analysis of the Homopolymers in Solution Produced during the Graft Polymerization of Glycidyl Methacrylate[a]

sample	grafting time t [h]	$[CPDB]_0$ [mmol/L]	number-average molecular mass, M_n [g/mol]	polydispersity, M_w/M_n	av number of monomer units/chain
a[b]	1	3.4	9×10^3	1.6	64
b	1	7.5	10×10^3	1.4	68
c	1	15.1	6×10^3	1.4	38
d	2	15.1	7×10^3	1.4	46
e	1		196×10^3	2.0	1380
f	2		229×10^3	1.9	1620

[a] RAFT-mediated produced homopolymers (samples a, b, c, and d) from a solution of methyl ethyl ketone (MEK) containing 2.93 mol/L of glycidyl methacrylate (GMA), 1 mmol/L of azobis(isobutyronitrile) (AIBN), and cyanoisopropyl dithiobenzoate (CPDB). Free radical polymerization produced homopolymers (samples e and f) from a solution of methyl ethyl ketone containing 2.93 mol/L of glycidyl methacrylate (GMA) and 1 mmol/L of azobis(isobutyronitrile) (AIBN). [b] For sample a the concentration of azobis(isobutyronitrile) (AIBN) was 0.5 mmol/L.

Diffraction Efficiency. The diffraction mask that was used in this study contained multiple gratings in order to be able to simultaneously expose interference patterns of different periodicity on the same polymer sample. The relative diffraction efficiency of these gratings into zeroth and first orders was measured using a charge coupled device (CCD) camera. The mask was placed at a distance of 5 cm to the CCD camera in order to get well-separated diffracted beams. The relative intensity of the diffracted beams was obtained from CCD images.

Reactions. *Free Radical Polymerization.* A 1 cm^2 ETFE sample was exposed at the XIL beamline to create nine fields with various patterns and different EUV exposure dose. The sample was then immersed in a 3 mL glass reactor tube containing 2.93 mol/L of glycidyl methacrylate in methyl ethyl ketone. The glass rector was sealed, and the solution was degassed with N_2 for 15 min. The reactor was placed in a preheated oil bath at a temperature of 70 °C for 30 min. The reactor was then opened, and the sample was removed. The sample was transferred into a cold acetone solution and sonicated for 1 h.

Analogous grafting experiments were carried out using 5−40% (v/v) of glycidyl methacrylate in isopropanol or methyl ethyl ketone. Reaction times were 30−120 min.

RAFT Polymerization. A 1 cm^2 sample exposed to EUV was immersed in a 3 mL glass reactor tube containing 2.93 mol/L of glycidyl methacrylate, 1 mmol/L of azobis(isobutyronitrile), and 15.1 mmol/L of cyanoisopropyl dithiobenzoate in methyl ethyl ketone. The glass rector was sealed, and the solution was degassed with N_2 for 15 min. The reactor was placed in a preheated oil bath at a temperature of 70 °C for 120 min. The reactor was then opened, and the sample was removed. The sample was transferred into a

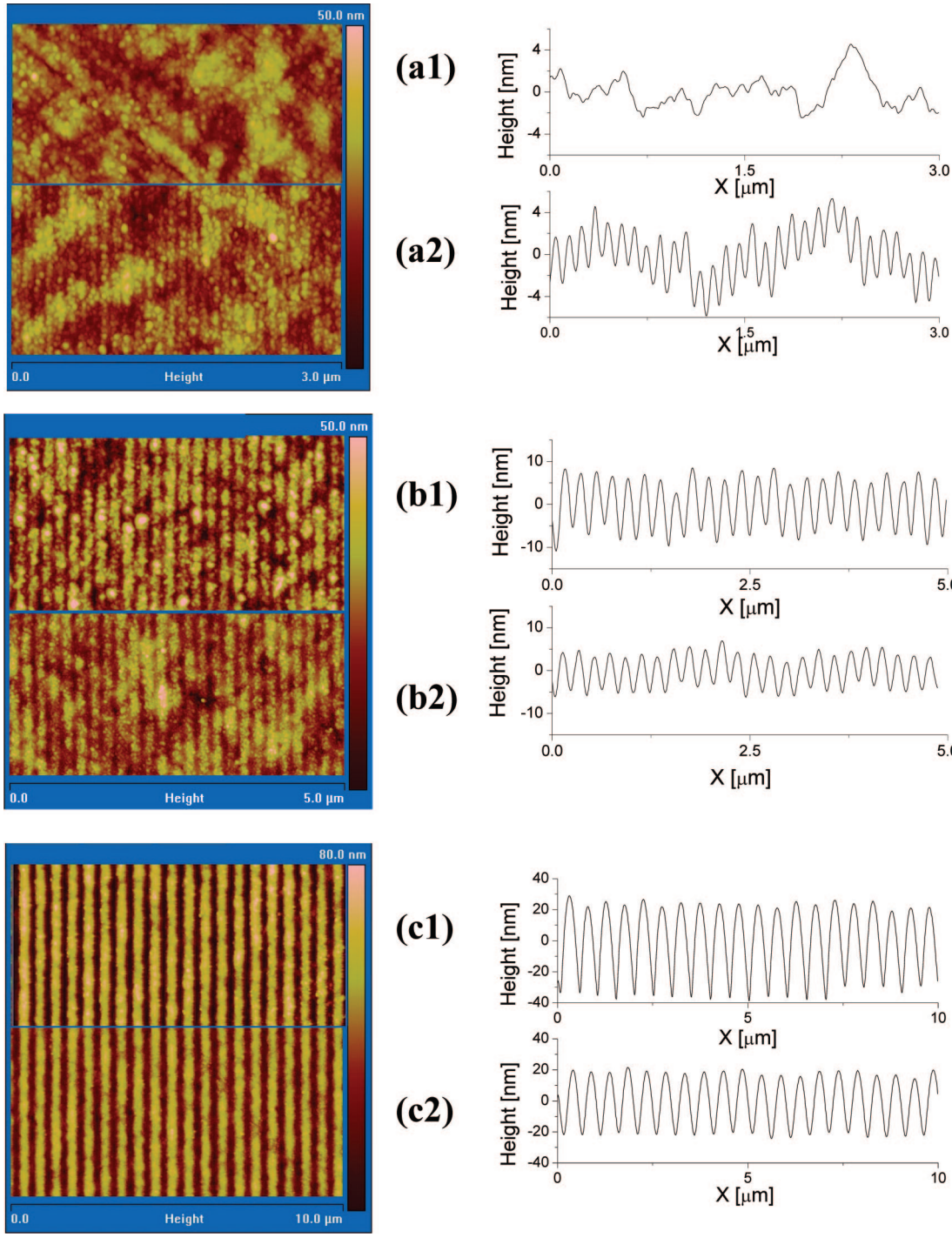

Figure 3. Atomic force microscopy images and line profiles of samples exposed with 6 mJ/cm^2 incident dose on the mask and grafted without (index 1) and with (index 2) the help of RAFT-mediated polymerization (2 h, with 15 mM of cyanoisopropyl dithiobenzoate and 1 mM of α,α′-azoisobutyronitrile): (a) 100 nm, (b) 200 nm, (c) 500 nm period lines. The upper part represents AFM pictures of samples grafted by the free radical mechanism.

cold acetone solution and sonicated for 1 h, whereas the polymerization solution was cooled down and the homopolymer formed in solution was precipitated using cold isopropanol for SEC analysis purposes (number-average molecular mass: 7000 g/mol; polydispersity: 1.4). In analogous experiments we varied the concentrations of CPBD between 3.4 and 15 mM and the monomer concentration of between 30 and 40% (v/v). The reaction times of 30−180 min were explored.

Characterization. Atomic force microscopy (AFM) was performed using a Digital Instrument Nanoscope III/Dimension 3100 in the tapping mode. Samples were mounted on glass slides or silicon wafers without any prior treatment. The height of the grafted layer was measured in the uniformly exposed areas.[43]

Scanning electron microscopy (SEM) was performed in a field-emission microscope (Zeiss SUPRA 55VP). The samples were sputter-coated with ~10 nm of gold to obtain sufficient conductivity.

The molecular weight distributions of homopolymers in the grafting solution were determined by triple detection size exclusion chromatography on a Viscotek TDA300 using two mixed bed columns (PSS (Germany) linear M SDV 8 × 300 5 μm) at a column temperature of 35 °C and at a flow of 1 mL/min of tetrahydrofuran (THF, GPC grade). The light scattering detection was performed

Table 2. Diffraction Efficiency of the Si_3N_4 Membrane/Chromium Gratings and Measured Structure Height

	diffraction efficiency of the mask [%]	absorbed dose[a] [mJ/cm^2]	av photon density [photons/nm^2]	av height for free radical polymerization[a] [nm]	av height for RAFT-mediated polymerization[a] [nm]
background noise	0.07	0.004	0.003		
zeroth order	52.6	3.16	2.14	1040 ± 50	150 ± 10
first order					
100 nm period lines	6.1	0.37	0.25	n.d	4 ± 1
200 nm period lines	8.5	0.51	0.35	15 ± 4	8 ± 2
500 nm period lines	10.2	0.61	0.41	60 ± 10	40 ± 5

[a] For 6 mJ/cm^2 incident dose on the mask.

at two scattering angles (7° and 90°), whereas the refractive index detection was done at a wavelength of 670 nm. Polymer samples were first dissolved in THF at a concentration of 10−20 mg/L and then injected in the SEC (sampling volume 100 μL).

PMMA standards (PSS ReadyCal PMMA standards (series) (800−1 180 000 g/mol)) were injected for calibration, and a specific refractive index increment (dn/dc) of 0.0935 mL/g[44,45] was used to calculate the absolute molar mass of pGMA polymers.

Results

Hot pressed 100 μm thick ETFE films were exposed at the EUV interference beamline in vacuum.[43] This irradiation step allows simultaneous writing of a series of uniformly exposed fields as well as nanostructures from the interference of the first-order diffracted beam on each sample. Irradiated samples were taken out of the vacuum chamber to allow the formation of stable peroxides from the radicals formed during the exposure on contact with the ambient air. Samples were then grafted with glycidyl methacrylate in methyl ethyl ketone following a "grafting from" process, where the polymer is grown step by step from dissociated peroxides, either by free radical polymerization or using the RAFT mechanism. The reaction temperature was brought to 70 °C within 2 min and induced polymerization by quick peroxide dissociation. In order to obtain well-resolved nanostructured patterns, grafting times were limited to 30 min for free radical and 2 h for RAFT-mediated polymerization. The grafting concentration was set to 30−40% of GMA to avoid substantial depletion at the growing ends of the grafted chains and to induce a homogeneous growth in all exposed areas of the film.

Dose Height Dependence. *a. Free Radical Polymerization.* First, the dose height dependence of the grafted GMA in MEK by free radical polymerization was investigated (Figure 2). The height of the grafted structures was measured by AFM in the uniformly exposed microstructured areas. We explored the dose range of 4−120 mJ/cm^2, as measured on the photodiode before the diffraction grating. The thickness of the grafted layer increases with the dose, assigned to an increase of the density of the brush, until a maximum of ~2.3 μm is reached at 50 mJ/cm^2 (Figure 2, curve a). Further increasing the dose decreases the brush thickness due to increased termination probability caused by the higher density of growing neighboring chains or due to radiation damage of the base polymer.[46]

b. RAFT-Mediated Polymerization. The fast grafting reaction of GMA by the free radical mechanism impedes a good control over the height of the grafted layer with the reaction time. In order to reduce the grafted layer thickness and to control the polymerization, we investigated the RAFT polymerization of GMA, mediated by CPDB as the chain transfer agent. The main idea of RAFT-mediated polymerization is based on the equilibrium between the growing chains and dormant species. In the investigated heterogeneous system, such an equilibrium can only be established if the polymerization takes place both at the surface and in the bulk solution. Therefore, AIBN was added in low concentration to the system to induce polymer chain growth also in the bulk solution. As an advantage of this parallel surface and bulk solution polymerization the length of polymer chains grown in solution can be analyzed by GPC and can give an indication on the length of polymer chains grown on the ETFE surface.

AIBN (1 mM) was first added to the system without any RAFT agent in order to create a reference. The measured grafted thickness (Figure 2, curve b) was substantially higher than for the "grafting from" method (Figure 2, curve a). The molecular mass (number-average (M_n)) of the polymer formed in solution was 196 000 g/mol for a 1 h grafting reaction (Table 1). The grafted layer should form by combination of "grafting from" and "grafting to" due to the fact that growing polymers created in solution can bind to the substrate or to already grafted polymer chains.

The concentration of AIBN was set to 1 mM in further experiments, and the RAFT chain transfer agent was set to 7.5 and 15 mM. The results are impressive, as by addition of RAFT chain transfer agent at low concentration (7.5 mM) the grafted thickness was diminished by a factor of 7 for a similar grafting time (Figure 2, curve c), compared to the one without RAFT chain transfer agent (Figure 2, curve b). The molecular mass of polymer formed in solution was drastically diminished by a factor of 20 (Table 1). When more RAFT chain transfer agent (15 mM) was added to the system (Figure 2, curve d), the effect was even more pronounced; the grafted thickness was again reduced by a factor of 4 for a similar reaction time. The molecular mass of the homopolymer formed in solution also diminished with the amount of RAFT chain transfer agent added to the system, but this effect was much less pronounced. The thickness of the grafted brush increased linearly with the grafting time; i.e., for a doubled reaction time twice thicker layers were measured (Figure 2, curves d and e). However, the molecular mass of polymers produced in solution increases only by ~20%.

Resolution of Nanostructures. Nanopatterns of radicals on ETFE films were created by the interference between first-order diffracted beams from the chromium gratings. Since the uniformly exposed areas and interference fields were simultaneously generated and grafted at identical conditions, similar molecular weight of the grafted polymer can be assumed in all exposed areas of the sample. RAFT-mediated polymerization should give shorter and less polydisperse polymer chains and, as a consequence, better-defined polymer nanostructures.

Three different line patterns with sinusoidal intensity distribution were investigated: a high-resolution one (100 nm period lines, Figure 3a), a medium-resolution one (200 nm period lines, Figure 3b), and a low-resolution one (500 nm period lines, Figure 3c). The radical patterns were written in one single exposure where the incident delivered dose measured on the photodiode was 6 mJ/cm^2. This dose was observed to be the optimum to get the best structure resolution. As measured with a CCD camera, the effective real absorbed dose in the interference areas was significantly lower due to photon absorption of the Si_3N_4 membrane and low diffraction efficiencies of the chromium grating (Table 2). The average doses delivered to the sample were 52.6% of the incident beam for the direct exposed area and 6−10% for the interference areas. These are average values for the interference region. Because of sinusoidal

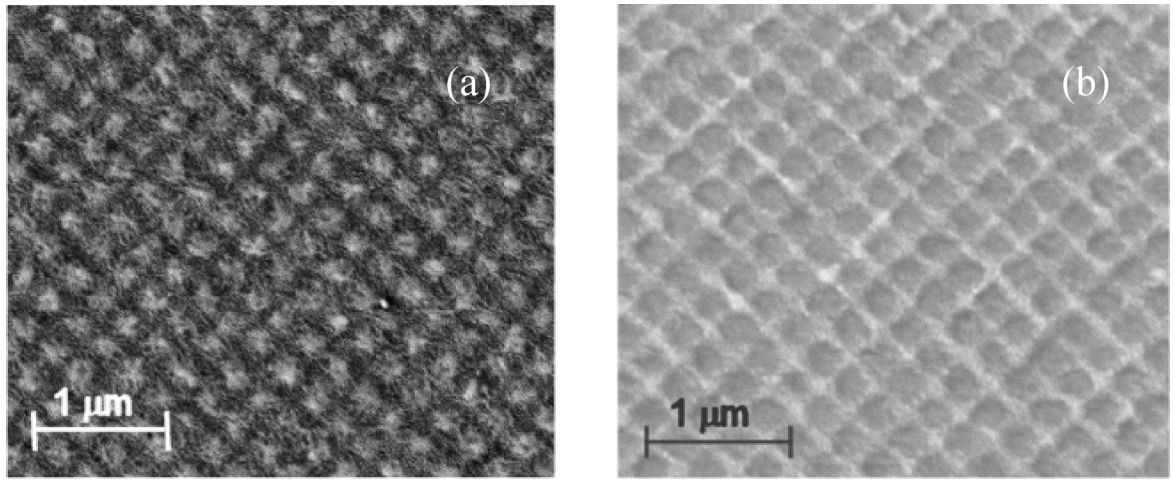

Figure 4. Scanning electron microscopic pictures of a four-beam interference pattern leading to 283 nm period dot pattern recorded (a) with the secondary electron detector (topographic contrast) and (b) with the in-lens detector (material contrast). The sample was exposed with 6 mJ/cm^2 incident dose and grafted for 2 h according to the RAFT mechanisms in 40% glycidyl methacrylate in methyl ethyl ketone containing 15 mM of cyanoisopropyl dithiobenzoate and 1 mM of α,α′-azoisobutyronitrile.

intensity distribution of the photons, the absorbed dose is twice higher at the amplitude maximum and near zero at the minimum amplitude.

For a similar deposited dose (6 mJ/cm^2, incident dose), the height measured in the uniformly exposed area (Figure 2) of samples grafted with RAFT-mediated polymerization were only 15% of the free radical grown ones (Table 2). In contrast, the height of features measured in the first-order diffraction area (Figure 3) was very similar (≈4 nm) for 100 nm period lines (Figure 3a) grown by the RAFT mechanism and by the free radical mechanism (Table 2). The main difference was that lines were only detected for RAFT grown samples, while grafted free radical grown polymer chains were scattered all over the sample. In both cases, polymers appear to be in a coiled state. The average coil diameter, presumably consisting of single grafted polymer chains, was determined from AFM measurements. The determined values were 29 ± 5 nm for the free radical polymerization and 21 ± 4 nm for RAFT-mediated polymerization.

The 200 and 500 nm patterns appear well resolved in both cases. For the 200 nm period lines (Figure 3b), free radical grown nanostructures were twice higher than RAFT ones (Table 2), whereas for the 500 nm period lines (Figure 3c), the height of the free radical grown lines were 50% higher than those fabricated by RAFT-mediated polymerization (Table 2). Polymer chains grafted in the 500 nm period lines (Figure 3c) appear to be in a brush regime, whereas grafted chains in the 200 nm period lines picture (Figure 3b) are in a mixed mushroom/brush state.

A 283 nm dot period pattern (Figure 4) of poly-GMA nanostructures synthesized via RAFT-mediated polymerization was investigated by SEM. The topographic picture taken with the secondary electron detector (Figure 4a) shows that the grafted polymer is composed of very long polymer chain bundles. Additionally, it reveals that the difference in grafting density between constructive (dots arrays) and destructive interferences is leading to a good topographical contrast. In the constructive inference areas the chains adopt a low-density brushlike structure, while in the destructive ones only scattered isolated polymer chains are found. The picture taken with the in-lens detector (Figure 4b), which is more sensitive to differences in chemical composition, reveals a good material contrast between the base fluoropolymer (bright) and the grafted poly-GMA (dark).

Discussion

Grafted uniformly exposed areas showed an increase of the grafted layer thickness with the dose. Assuming that initiation, propagation, and termination rates of surface grown chains are similar for all the investigated densities of preformed radicals, the regular height increase of the grafted layer thickness with increasing dose must be caused by a strong stretching of the grafted chains. Polymer chains grafted in the uniformly exposed areas are therefore in a highly stretched brush state for both free radical and RAFT-mediated polymerization.

RAFT-meditated polymerization gave, as expected from the literature, lower grafted thickness compared to free radical polymerization (Figure 2). But, in contrast to literature reports on grafting from immobilized initiators,[29] the polymer chains grown from the surface are longer than those formed simultaneously in the solution. For example, for the case of the 1 h grafting experiment with 7.5 mM of RAFT chain transfer agent in the solution, M_n of the polymer formed in the bulk solution was 10 000 g/mol, which corresponds to about 70 monomer units. Considering that the distance between two monomer units is ∼2.5 Å, the graft layer thickness should not exceed 18 nm when grafted polymer chains are in a fully stretched conformation. In our case, the grafted layer thickness is on the order of 1 μm (Figure 2, curve c). We therefore assume that the kinetics of RAFT-mediated reaction is different on the surface and in solution. We previously discovered that the initiation rates and termination rates of the grafting reactions are highly affected by the viscosity of the system.[46] The higher the viscosity in the initial polymerization solution, the lower the termination rates and the thicker the grafted layer is. The production of homopolymer in the solution and their affinity for the grafted layer implies that the viscosity within the grafted layer is much higher than in solution. These highly viscose regions create very local Trommsdorff effects where termination rates are reduced by the lack of mobility of surface grown chains.[46]

A mushroom to brush transition was observed at the AFM between grafted chains in the 100 and 500 nm period line nanostructures. We assumed that for low-, medium-, and high-resolution lines polymer chains possess a similar molecular weight for a single grafting batch. From the height of the 100 nm period lines of less than 5 nm it is concluded that polymers are in a typical coiled state for both RAFT-mediated and free radical polymerization (Figure 3a). In the free radical polymerization, long polymer chains are grown at a low surface

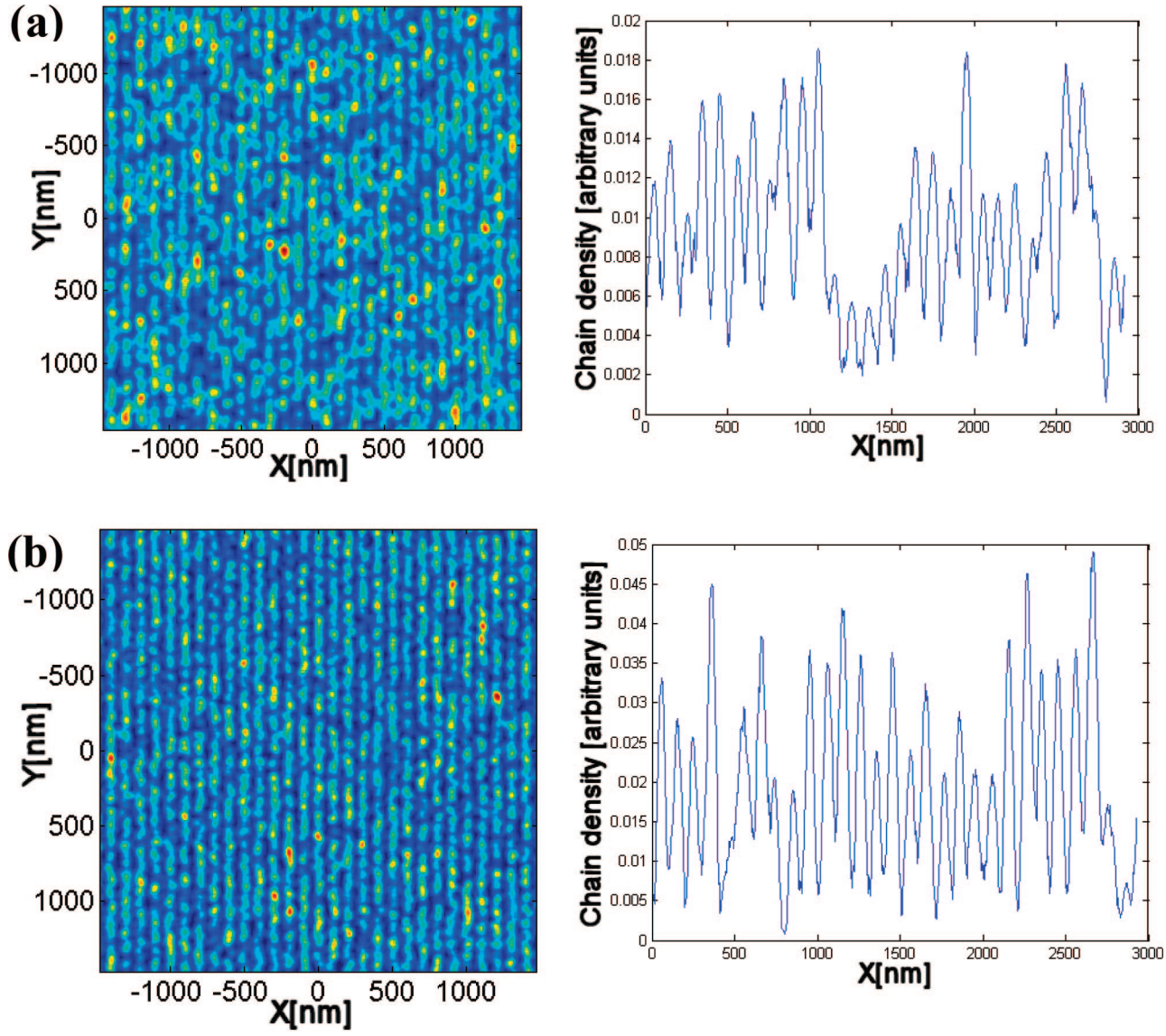

Figure 5. Simulated pictures and line profiles of 100 period lines for an incident dose on the mask of 6 mJ/cm^2, for grafting of glycidyl methacrylate by free-radical (a) and RAFT-mediated graft polymerization (b).

density, leading to poor structure definition. RAFT-mediated grafting of 100 nm period lines lead to shorter polymer chains that adopt a coiled conformation with 4 nm in height. Since the measured average coiled diameter of a single surface grown polymer chain was in the range of 20−30 nm for both polymerization mechanisms with an average height of ∼4 nm at low grafting density, the molecular mass of surface grown polymer is expected to be in the million dalton range. Interestingly, this high molecular mass matches the measured grafted height obtained in the uniformly exposed areas at high dose (Figure 2) and the SEM observations (Figure 4).

In AFM images of 200 nm period lines, patterns appear nicely resolved for both polymerization schemes. Following similar assumption as for the 100 nm period lines the difference in height (≈7 nm) between free radical and RAFT grown polymer is then primarily explained by higher molecular weight of free radical grafted polymers. For the 200 nm line pattern, it appears that polymers are in a transition state between the mushroom and the brush regime, where the radius of gyration of grafted polymer chains and the distance between two grafted chains are of very similar value.

For the 500 nm period lines, patterns are very well resolved. The grafted height is 10 times higher than for the 100 nm period lines, with a 1.7 times higher absorbed dose. For both grafting paths, the grafted polymer chains appear to be sufficiently dense packed to adopt a stretched brush conformation.

The requirement to obtain a stretching of surface grafted polymers is that the individual coils overlap. From our measurements of the coiled size of single polymer chains (29 ± 5 nm, free radical; 21 ± 4 nm, RAFT) we calculated the density (D_o) required to get overlapping coils according to the equation

$$D_o = \frac{1}{A} \tag{1}$$

where A is the planar surface area of a single coiled chain. A minimum density (D_o) of (1.5 ± 0.7) × 10^{-3} and (3 ± 1.3) × 10^{-3} chains/nm^2 should be reached to obtain overlapping coils for the free radical case and RAFT-mediated polymerization, respectively. The calculated lower density of free radical polymerization is compensated with a higher molecular weight of the grafted polymers, so that the transition mushrooms/brush occurs at a lower grafted density than for shorter polymers produced by RAFT-mediated polymerization. Since a typical polymer brush is observed for 500 nm period lines (Figure 3c) as a mixed mushroom/brush state is reached for the 200 nm line period (Figure 3b), the transition from mushrooms to brush

appears to occur for an absorbed dose between 0.5 and 0.6 mJ/cm^2 corresponding to an average absorbed photon density (D_{ph}) between 0.35 and 0.41 photons/nm^2 (Table 2). An overall photon conversion efficiency (η) can be defined as the ratio between the calculated minimum overlapping density (D_o) and the absorbed photon density (D_{ph}) at the observed corresponding mushroom to brush transition:

$$\eta = \frac{D_o}{D_{ph}} \tag{2}$$

The ratio η also denotes the fraction of photons absorbed by the polymer backbone that starts a polymer chain. It was calculate to be as low as 0.4 ± 0.2% for the free radical polymerization mechanism and 0.8 ± 0.5% for the RAFT-mediated case.

The absorbed dose in the uniformly exposed area was much higher than those in the interference areas for a similar incident dose on the mask (Table 2). Assuming that η stays constant with increasing dose and within a reaction batch, an average chain density of 8.8×10^{-3} chains/nm^2 and 16.4×10^{-3} chains/nm^2 can be calculated for the uniformly exposed area (6 mJ/cm^2), which is far beyond the mushroom to brush threshold. Grafted polymers are forced to stretch away from the surface, resulting in a thickness of the brush layer as high as 1 μm for the free radical case and 200 nm for the RAFT-mediated case. The maximum height of the grafted layer is therefore also the maximum achievable grafting density. For the free radical case ~0.1 chains/nm^2 were packed at 50 mJ/cm^2 incident dose on the photodiode (Figure 2), as for RAFT-mediated polymerization ~0.2 chains/nm^2 were grafted at 50 mJ/cm^2.

Simulation of Sinusoidal Line Profiles. The utilizable dose range to get well-resolved interference patterns is low compared to uniformly exposed samples (Table 2). At such low dose, single photon events have to be considered for the formation of the nanostructures. A simulation was performed to determine the effect of photon statistics on the resolution of 100 nm nanostructure patterns. It was realized using a Poisson distribution to create sinusoidal intensity profiles. To match with our experimental data we had to make some assumptions. (i)The dose delivered in the 100 nm interference pattern was corrected according to the measured efficiency of the mask (Table 2). (ii)For the free radical polymerization it was assumed based on our calculation that η was 0.4%. For RAFT polymerization the initiation is more efficient: η = 0.8% was used for the simulation. (iii)The diameter of one coiled polymer chain based on our AFM measurements is 29 nm when grown by free radical mechanism and 21 nm when grafted by RAFT-mediated polymerization. The shape of each coil was approximated with a rotationally symmetrical Gaussian curve.

Photon statistical simulations were performed for an incident delivered dose on the mask of 6 mJ/cm^2 (Table 2). The simulated results for 100 nm are shown in Figure 5 and match perfectly with the AFM measured 100 nm period lines (Figure 3a). The effect of photon statistics is much more pronounced for the free radical polymerization due to the lower initiation efficiency. The big coil size of surface grown polymers, in the order of the line feature width, limits the resolution of the pattern by merging the lines together. This effect is more pronounced for free radical polymerization (Figure 5a) where the size of the coiled polymer is bigger than for the RAFT-mediated polymerization (Figure 5b).

The limited resolution of the 100 nm period lines is determined by the poor photon statistics at low dose as well as by the huge size of the grafted chains. Increasing the number of photons could be used to improve the statistics; however, it decreases the pattern resolution because of merging polymer chains.

Conclusions and Outlook

RAFT polymerization is a versatile method to control grafting of polymers onto EUV-exposed fluoropolymers as it allows to control the polymer chain length and to enhance the resolution of nanostructured line patterns into the 50 nm range. The sensitivity of the grafting process is rather high compared to standard EUV lithographic methods; however, less than 1% of the preformed radicals can start a polymer chain. A high-density polymer brush with 0.1−0.2 chains/nm^2 was obtained from high-dose-exposed samples. However, low doses had to be applied to avoid bridging of the nanoscale features by the high-molecular-weight grafted polymer chains. As a consequence, the ultimate resolution limit is determined by photon statistics. In order to increase the resolution, higher dose has to be delivered on the interference pattern and more effort has to put into grafting even shorter polymer chains to avoid bridging between the line features.

Acknowledgment. The authors thank Konrad Vogelsang, Sandro Bellini, and Rolf Schelldorfer for their technical support and Dominique Desbouis for fruitful discussions. EUV interference lithographic exposures reported in this work were performed at the Swiss Light Source, Paul Scherrer Institut, Villigen, Switzerland.

References and Notes

(1) Advincula, R.; Brittain, W. J.; Caster, K. C.; Rühe, J. *Polymer Brushes: Synthesis, Characterization, Applications*; Wiley-VCH: Weinheim, 2004.
(2) Alexander, S. *J. Phys. (Paris)* **1977**, *38* (8), 977–981.
(3) Lai, P. Y.; Halperin, A. *Macromolecules* **1991**, *24* (17), 4981–4982.
(4) Milner, S. T. *Science* **1991**, *251* (4996), 905–914.
(5) Milner, S. T.; Witten, T. A.; Cates, M. E. *Macromolecules* **1988**, *21* (8), 2610–2619.
(6) Patra, M.; Linse, P. *Nano Lett.* **2006**, *6* (1), 133–137.
(7) Yamamoto, S.; Ejaz, M.; Tsujii, Y.; Fukuda, T. *Macromolecules* **2000**, *33* (15), 5608–5612.
(8) Yamamoto, S.; Ejaz, M.; Tsujii, Y.; Matsumoto, M.; Fukuda, T. *Macromolecules* **2000**, *33* (15), 5602–5607.
(9) Jordan, R. *Surface-Initiated Polymerization I*; Springer: Berlin, 2006.
(10) Jordan, R. *Surface-Initiated Polymerization II*; Springer: Berlin, 2006.
(11) Uyama, Y.; Kato, K.; Ikada, Y. *Adv. Polym. Sci.* **1998**, *137*, 1–39.
(12) Zhao, B.; Brittain, W. J. *Prog. Polym. Sci.* **2000**, *25* (5), 677–710.
(13) Li, J.; Zhai, M. L.; Yi, M.; Gao, H. C.; Ha, H. F. *Radiat. Phys. Chem.* **1999**, *55* (2), 173–178.
(14) Omichi, H. *Nucl. Instrum. Methods Phys. Res., Sect. B* **1995**, *105* (1−4), 302–307.
(15) Prucker, O.; Ruhe, J. *Langmuir* **1998**, *14* (24), 6893–6898.
(16) Edmondson, S.; Osborne, V. L.; Huck, W. T. S. *Chem. Soc. Rev.* **2004**, *33* (1), 14–22.
(17) Pyun, J.; Kowalewski, T.; Matyjaszewski, K. *Macromol. Rapid Commun.* **2003**, *24* (18), 1043–1059.
(18) Dargaville, T. R. *Prog. Polym. Sci.* **2003**, *28* (9), 1355–1376.
(19) Desai, S. M. *Long-Term Prop. Polyolefins* **2004**, *169*, 231–293.
(20) Liu, P. *e-Polym.* **2007**.
(21) Husseman, M.; Malmstrom, E. E.; McNamara, M.; Mate, M.; Mecerreyes, D.; Benoit, D. G.; Hedrick, J. L.; Mansky, P.; Huang, E.; Russell, T. P.; Hawker, C. J. *Macromolecules* **1999**, *32* (5), 1424–1431.
(22) Miwa, Y.; Yamamoto, K.; Sakaguchi, M.; Shimada, S. *Macromolecules* **1999**, *32* (24), 8234–8236.
(23) Sugino, Y.; Yamamoto, K.; Miwa, Y.; Sakaguchi, M.; Shimada, S. *e-Polym.* **2003**, 8.
(24) Yamamoto, K.; Nakazono, M.; Miwa, Y.; Hara, S.; Sakaguchi, M.; Shimada, S. *Polym. J.* **2001**, *33* (11), 862–867.
(25) Desai, S. M.; Solanky, S. S.; Mandale, A. B.; Rathore, K.; Singh, R. P. *Polymer* **2003**, *44* (25), 7645–7649.
(26) Ejaz, M.; Yamamoto, S.; Ohno, K.; Tsujii, Y.; Fukuda, T. *Macromolecules* **1998**, *31* (17), 5934–5936.
(27) Yamamoto, K.; Miwa, Y.; Tanaka, H.; Sakaguchi, M.; Shimada, S. *J. Polym. Sci., Part A: Polym. Chem.* **2002**, *40* (20), 3350–3359.
(28) Baum, M.; Brittain, W. J. *Macromolecules* **2002**, *35* (3), 610–615.
(29) Tsujii, Y.; Ejaz, M.; Sato, K.; Goto, A.; Fukuda, T. *Macromolecules* **2001**, *34* (26), 8872–8878.
(30) Yoshikawa, C.; Goto, A.; Tsujii, Y.; Fukuda, T.; Yamamoto, K.; Kishida, A. *Macromolecules* **2005**, *38* (11), 4604–4610.
(31) Farhan, T.; Huck, W. T. S. *Eur. Polym. J.* **2004**, *40* (8), 1599–1604.

(32) Gölzhauser, A.; Eck, W.; Geyer, W.; Stadler, V.; Weimann, T.; Hinze, P.; Grunze, M. *Adv. Mater.* **2001**, *13* (11), 803–806.
(33) Husemann, M.; Mecerreyes, D.; Hawker, C. J.; Hedrick, J. L.; Shah, R.; Abbott, N. L. *Angew. Chem., Int. Ed.* **1999**, *38* (5), 647–649.
(34) Liu, G. Y.; Xu, S.; Qian, Y. L. *Acc. Chem. Res.* **2000**, *33* (7), 457–466.
(35) Piner, R. D.; Zhu, J.; Xu, F.; Hong, S. H.; Mirkin, C. A. *Science* **1999**, *283* (5402), 661–663.
(36) Rühe, J. *Macromol. Symp.* **1997**, *126*, 215–222.
(37) Shah, R. R.; Merreceyes, D.; Husemann, M.; Rees, I.; Abbott, N. L.; Hawker, C. J.; Hedrick, J. L. *Macromolecules* **2000**, *33* (2), 597–605.
(38) Brack, H. P.; Padeste, C.; Slaski, M.; Alkan, S.; Solak, H. H. *J. Am. Chem. Soc.* **2004**, *126* (4), 1004–1005.
(39) Solak, H. H. *J. Phys. D: Appl. Phys.* **2006**, *39* (10), R171−R188.
(40) Padeste, C.; Farquet, P.; Potzner, C.; Solak, H. H. *J. Biomater. Sci., Polym. Ed.* **2006**, *17* (11), 1285–1300.
(41) Dureault, A.; Gnanou, Y.; Taton, D.; Destarac, M.; Leising, F. *Angew. Chem., Int. Ed.* **2003**, *42* (25), 2869–2872.
(42) Padeste, C.; Solak, H. H.; Brack, H. P.; Slaski, M.; Gursel, S. A.; Scherer, G. G. *J. Vac. Sci. Technol. B* **2004**, *22* (6), 3191–3195.
(43) Solak, H. H.; David, C.; Gobrecht, J.; Golovkina, V.; Cerrina, F.; Kim, S. O.; Nealey, P. F. *Microelectron. Eng.* **2003**, *67−8*, 56–62.
(44) Mrkvickova, L.; Kalal, J.; Bednar, B.; Janca, J. *Makromol. Chem.* **1982**, *183* (1), 203–210.
(45) Virtanen, J.; Tenhu, H. *J. Polym. Sci., Part A: Polym. Chem.* **2001**, *39* (21), 3716–3725.
(46) Farquet, P.; Kunze, A.; Padeste, C.; Solak, H. H.; Gursel, S. A.; Scherer, G. G.; Wokaun, A. *Polymer* **2007**, *48* (17), 49364942.

MA800202B